Arch. Metall. Mater. **69** (2024), 4, 1367-1373

DOI: https://doi.org/10.24425/amm.2024.151401

V. ÖZKAN BILICI[1*], A. YÖNETKEN[2], A. EROL[3]

USE OF ULTRASOUND TO IDENTIFY MICROSTRUCTURE-PROPERTY RELATIONSHIPS IN (AlN + WC) FABRICATED WITH ELECTROLESS NI PRODUCING

In order to improve the properties of the materials produced by the powder metallurgy method, first of all, powders (16.59% AlN + 6.63% WC) were coated with nickel (Ni) by electroless method, and then box boriding, which is one of the most widely used surface coating methods, was applied. A composite formed with (16.59% AlN + 6.63% WC)76.7Ni was prepared under the Ar shroud in the temperature range of 1000-1400°C. Pulse-echo technique was used for ultrasonic velocity measurements on Ni coated (16.59% AlN + 6.63% WC) samples. It is aimed to examine the change of physical, mechanical and ultrasonic properties of the obtained ceramic-metal composites depending on different sintering temperatures. In addition, the samples were characterized by mechanical and metallographic examination. The results show that the longitudinal and transverse ultrasonic velocity values and ultrasonic modulus (shear, bulk, Young's etc.) values increase simultaneously with the increase of sintering temperature. The highest microhardness value was observed in composite samples sintered at 1400°C and its value was 1150.80 Hv. The increased strength is mainly due to grain refinement and strong interfacial bonding between Ni particles and AlN and WC matrix.

Keywords: Ultrasonic measurements; Pulse-Echo; Powder Metallurgy; Electroless Nickel Plating; Boriding

1. Introduction

In order to improve the mechanical and microstructural properties of ceramic materials, ceramic matrix composites with metal particles are obtained by mixing with metal powders in the classical powder metallurgy method [1]. One of the coating techniques used in the production of ceramic metal composites is the electroless nickel plating method. With this coating, more robust, durable, corrosion and wear resistant materials are obtained. The biggest advantage of electroless nickel plating is that apart from the fact that it covers the entire surface of a piece, the powders are homogeneous and fine in size at the end of the plating process. [2-7]. In recent years, besides the studies on electroless nickel coatings, it has shifted to (Ni-B) coatings with the inclusion of boron coating [8-10]. One of the new application areas of boron and boron derivative products, which have hundreds of different uses, is their use as a kind of surface hardening method in steels, cast irons, nickel alloys, titanium alloys and sintered carbides. Compared to traditional hardening methods, boriding has many advantages. The boride layer formed on the surface is one of the most important advantages of this method, as it has high microhardness values and maintains its microhardness at high temperatures, as well as having superior properties such as good wear, oxidation and corrosion resistance [11-12]. While there is more than one method to measure the elastic modulus, "non-destructive" testing methods are preferred more as an alternative. The most preferred of these non-destructive methods is the ultrasonic pulse-echo method, which has high accuracy and is measured without damaging the tested material [13-16]. The transverse and longitudinal wave velocities in the materials are measured and then the elasticity model is used to calculate the elastic modulus [17-18].

In order to increase the strength and improve other properties of the composites produced in this study, first nickel plated with electroless coating method and then box boriding. This study aimed to investigate the elastic properties of "(16.59% AlN + 6.63% WC)76.7Ni" composites depending on different sintering temperature using ultrasonic bulk wave velocity properties. In addition, it is aimed to evaluate the mechanical properties of the produced composite samples depending on the sintering temperature.

[1] AFYON KOCATEPE UNIVERSITY, SCIENCE AND LITERATURE FACULTY, PHYSICS DEPT., 03200, AFYONKARAHISAR, TURKEY
[2] AFYON KOCATEPE UNIVERSITY, ENGINEERING FACULTY, ELECTRICAL ENGINEERING DEPT., 03200, AFYONKARAHISAR, TURKEY
[3] AFYON KOCATEPE UNIVERSITY, TECHNOLOGY FACULTY, METALLURGY AND MATERIALS ENGINEERING DEPT., 03200, AFYONKARAHISAR, TURKEY
* Corresponding author: vildanozkan@aku.edu.tr

2. Materials and methods

In this study; WC powder of 99.8% purity and 10 µm size from Aldrich and AlN with 99% purity and –325 mesh size were obtained from Aldrich company. WC and AlN powders were subjected to Ni plating process using hydrazine bath with electroless Ni plating technique. Nickel Chloride, Hydrazine Hydrate ($N_2H_4.H_2O$) and 30 vol.% Ammonia was used in the plating bath ($NiCI_2.6H_2O$).

During the coating, the bath temperature was kept constant at 90-95°C and the pH value was measured between 9-10 by Philips brand PW 9413 Ion-Activity Meter. The coated powders were washed several times with distilled water and alcohol and filtered by removing the residues remaining from the coating. The coated powders were dried in an oven at 105°C for 24 hours. The coated powders were shaped in a cylindrical mold under 300 bar pressure in a uniaxial hydraulic press. The shaped samples were sintered in a conventional sintering furnace for one hour in Argon atmosphere at temperatures of 1000-1400°C and composites were produced by powder metallurgy. Composite specimen dimensions were taken as 0.12" (3 mm) thickness and 0.6" (15 mm) diameter for all tests. Five samples per volume fraction were tested for all manufactured composites. After the physical and metallographic examinations of the produced composite samples, the box boriding process was applied at 950°C for 4 hours. Ecrit powder was used to prevent oxidation in boriding samples produced as (16.59% AlN + 6.63% WC)76Ni. For metallographic measurements, LEO 1430 VP model Scanning electron microscope and H Oxford EDX analyzer were used for microstructure examinations and the density Sample densities were calculated according to the Archimedes principle. The microhardness of boriding samples were measured. Nickel plating bath chemicals and their ratios are given in TABLE 1.

TABLE 1

Nickel plating bath and ratios

Chemical	Raitos
Aluminum nitride (AlN)	12
Tungsten carbide (WC)	1 g
Nickel chloride ($NiCI_2.6H_2O$) in powder form	72 g
Hydrazine hydrate ($N_2H_4.H_2O$)	20%
Distilled water	80%
Temperature (°C)	90-100 (°C)
pH values	8-10

3. Elastic property measurement using ultrasonic wave velocities

In the ultrasonic pulse echo technique, an ultrasound wave is excited by a piezoelectric transducer (transmitter and receiver) and sent into the material. The ultrasonic velocity is determined by the known thickness (d) of the samples, (Δt) which is the difference between the time the wave hits the surface of the sample and the second (transition time) when it leaves the other side [19]. In short, velocity is expressed as the distance (thickness of the sample) divided by the time delay.

The ultrasonic velocity of the wave is equal to:

$$V = \frac{2 \times d}{\Delta t} \tag{1}$$

where d is the thickness and Δt is the time delay [20-21].

Sonatest Sitescan 150 Pulser/Receiver device was used with pulse echo method, which is one of the ultrasonic measurement methods, to measure ultrasonic velocity values of samples sintered at different temperatures. The center frequencies of the probes are 2 MHz for longitudinal waves and 4 MHz for transverse waves. The thickness of the samples was measured with a caliper (with an accuracy of 0.01 mm). Ultrasonic longitudinal and transverse wave velocities (V_L and V_S) together with parameters such as elastic modulus (Y: Young's modulus, G: shear modulus and K: volume modulus) can be determined with the following expressions [22-27].

$$E = \rho V_T^2 \frac{3V_L^2 - 4V_T^2}{V_L^2 - V_T^2} \tag{2}$$

$$G = \rho V_T^2 \tag{3}$$

$$K = \frac{\rho}{3} 3V_L^2 - 4V_T^2 \tag{4}$$

Here, the E, G, K and ρ values are Young's (elastic) modulus, shear (stiffness) modulus, bulk modulus and density of the sample, respectively. All measurements were repeated at least three times and are reported in TABLE 2 with the mean ± one standard deviation. For composites (16.59% AlN + 6.63% WC) 76.7Ni, measurements were performed both along the thickness and along the layers (lateral direction). The coordinate system and the schematic representation of the experimental setup used for ultrasonic analysis are described in Fig. 1.

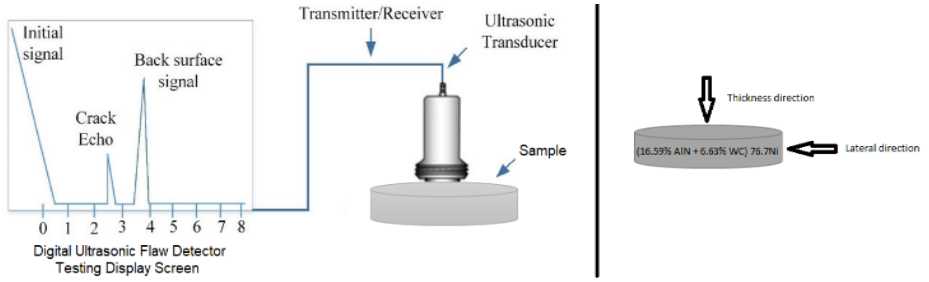

Fig. 1. Schematic diagram of the ultrasonic testing (UT) experiment set-up, depicting the test screen and definition of the coordinate system for ultrasonic analysis

4. Mechanical and metallographic examination

Ceramic-metal composite samples produced by powder metallurgy were nickel-plated with electroless nickel plating technique and sintered in an argon atmosphere at temperatures of 1000-1400°C. The sintered samples were then boriding by box drilling at 950°C for 4 hours. The densities of the boriding composite samples were calculated according to Archimedes' law, the greater the density of the liquid, the higher it will lift the hydrometer and the less the part of the instrument immersed in the liquid will be. The number read across the division line of the hydrometer standing in equilibrium in a liquid, which coincides with the liquid surface, gives the density of that liquid.

After the ceramic-metal composite samples produced with electroless nickel plating were sintered at 1000-1100-1200-1300-1400°C in an argon atmosphere, the microhardness of the boriding composite samples was measured in Vickers with a Shimadzu HMV 2L microhardness device. Its application areas are metal, ceramic and plastic materials, and it is a device that can apply loads from 10 gr to 2 kg. Both sides of the prepared samples are flat and smooth. The surface to be measured is polished. Microhardness measurements were made at 10 different points and microhardness measurements were obtained by taking the average of the microhardness values. At the same time, metallographic examination was carried out in order to understand the compounds, sequences and material structure of the boriding sample after electroless nickel plating with powder metallurgy. Boriding (16.59% AlN + 6.63% WC)76.7Ni composite samples were metallographically used in microstructure studies with LEO 1430 VP model Scanning electron microscope and Oxford EDX analyzer. Boriding samples are characterized by XRD analysis.

4.1. X-Ray Diffraction Analysis

At the highest sintered temperature, the grain boundaries became more pronounced and the surface open porosity decreased. (16.59% AlN + 6.63% WC) 76.7Ni X-Ray analysis results of 1400°C composite revealed WC, AlN ceramic phases as well as Ni metallic phase, respectively. In addition to the ceramic metal phases, Ni_3B, Ni_4B_3 and Ni_2B were determined as metallic boride phases. Controlling the C/W ratio is vital for the characteristics of the WC. Even slight deviations from the ideal carbon content result in the formation of either graphite or W_2C phases. If there is more than a stoichiometric amount of W dust, W_2C is formed according to the following equivalence. It is assumed that the metallic tungsten formed then undergoes the following reactions to form tungsten carbide:

$$W + C \rightarrow WC \quad (5)$$

$$W + 0.5\ C \rightarrow W_2C \quad (6)$$

$$W_2C + C \rightarrow 2WC \quad (7)$$

$$WC + W \rightarrow W_2C \quad (8)$$

This reaction takes place around 1250°C. It is known to decompose into W_2C, WC and W components below this temperature [28-30]. As a result of the experiments, it was seen that the tungsten peaks were less in the samples with high temperature in the XRD analysis. In addition, the amount of carbon decreases due to the oxidation of carbon during sintering, and as a result of the exothermic reaction with other elements in the vacuum environment during sintering, the amount of WC phase decreased and Ni_3B_4 phase emerged.

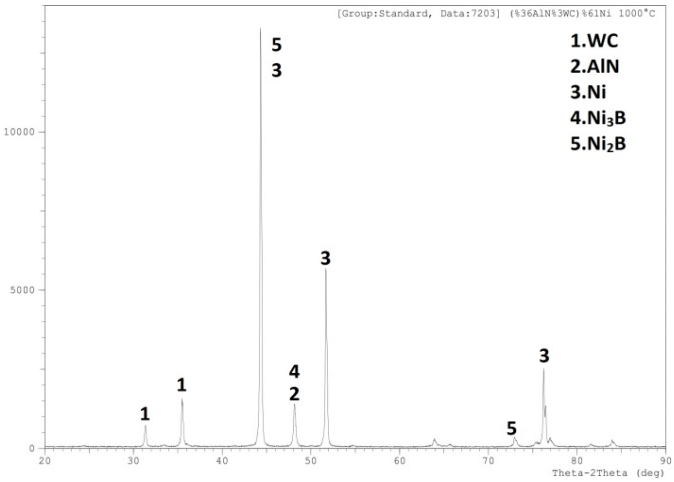

Fig. 2. X-Ray Diffraction diffractograms of (16.59% AlN + 6.63% WC)76.7Ni composite at 1000°C

X-ray analysis of samples sintered at 1000°C and then boronized is given in Fig. 2. Obtaining boron phases in samples sintered at 1000°C shows that boronization has taken place.

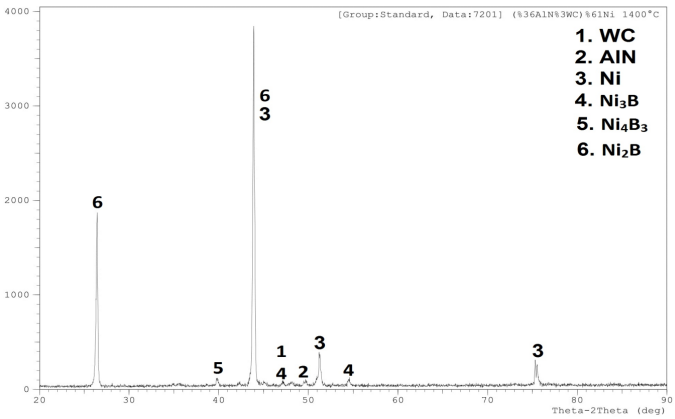

Fig. 3. X-Ray Diffraction diffractograms of (16.59% AlN + 6.63% WC)76.7Ni composite at 1400°C

In Fig. 3, grain coarsening was observed with increasing sintering temperature in (16.59% AlN + 6.63% WC)76.7Ni composites. In the X-Ray analysis results of the 1400°C composite, along with the phases showing the presence of WC, AlN, Ni powders used in the study, many intermetallic phases such as Ni_3B, Ni_2B and Ni_4B_3 are formed between nickel and boron with the effect of boriding.

4.2. SEM Analysis

The thickness of the Ni coating deposited on the surface of the powder particles after Electroless Ni coating of the powders was measured as 1-2 μm. The Ni coating thickness in the coated samples was molded under pressure after the Electroless Ni coating process. Afterwards, the precipitation thickness around the particles was measured in SEM images. Surface morphology images of samples produced at 1000°C and 1400°C of composition (16.59% AlN + 6.63% WC)76Ni with a scanning electron microscope (SEM) focused beam of electrons are given Fig. 4, surface SEM micrographs of the samples that were sintered at 1000°C and then boriding process were given. Microstructure differences are observed in the samples sintered at 1000°C, due to the fact that the bonding of the particles is weaker than the sample sintered at 1400°C depending on the temperature and its porosity is higher.

SEM micrographs of the surface of the samples sintered at 1400°C and then borided are given in Fig. 5. In the samples sintered at 1400°C, the bond formation of the particles with each other was better. The low porosity indicates that the boriding process is performed better. The appearance of acicular slices in the sample microstructures supports its high hardness.

5. Results

Ultrasonic longitudinal and transverse wave velocities, Young's modulus, shear modulus, bulk modulus, microhardness and density measurement results of sintered (16.59% AlN + 6.63% WC) 76.7Ni ceramic-metal composite samples are shown in TABLE 2. Graphs were drawn depending on the sintering temperature to understand whether their interactions and existing relationships with each other are significant. Looking

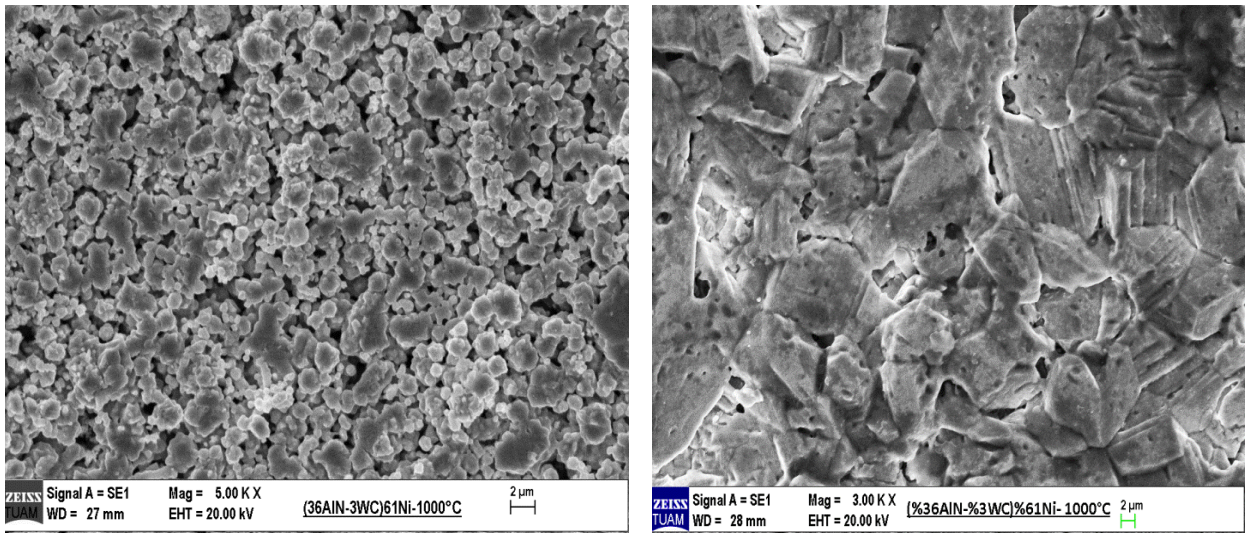

a) Unborided sample b) Borided sample

Fig. 4. SEM micrographs of (16.59% AlN + 6.63% WC)76.7Ni composite at 1000°C

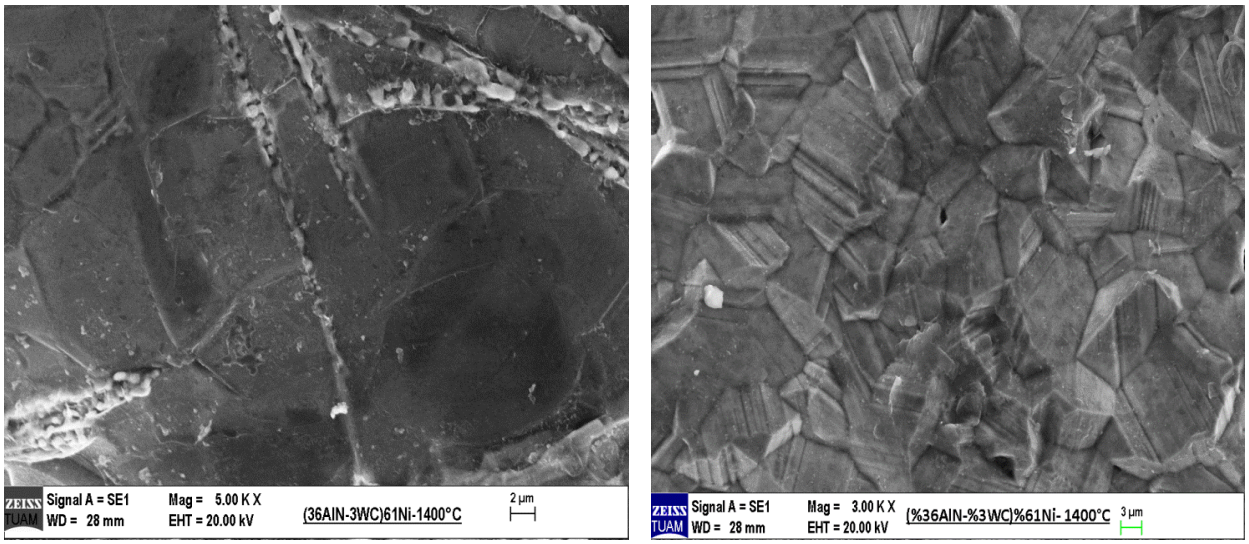

a) Unborided sample b) Borided sample

Fig. 5. SEM micrographs of (16.59% AlN + 6.63% WC)76.7Ni composite at 1400°C

TABLE 2

Ultrasonic, mechanical properties and sintering temperatures of ceramic-metal composites

Composite Samples	Sintering Temperature (°C)	Longitudinal Velocity (m/s)	Transverse Velocity (m/s)	Young's Modulus (GPa)	Shear Modulus (GPa)	Bulk Modulus (GPa)	Density (g/cm^3)	Microhardness HV (0.3)
(16.59% AlN + 6.63% WC) 76.7Ni	1000	2443±33.9	1200±11.3	21.82	8.14	22.87	5.65±0.1	285.3±21.3
	1100	3159±60.1	1403±31.1	33.83	12.28	45.89	6.24±0.11	554.9±34.7
	1200	3330±5.7	1637±36.8	47.14	17.58	49.30	6.56±0.13	589.6±32.4
	1300	3438±6.4	1756±60.1	59.09	22.33	55.81	7.24±0.12	975.3±45.6
	1400	3743±12.7	1880±14.1	69.83	26.23	68.99	7.42±012	1150.8±56.1

at the graphics, it is seen that the sintering temperature is effective in the composite structure to be formed and the ultrasonic longitudinal and transverse wave velocity increases with its increase. Fig. 6 shows the evolution of Young's modulus, shear modulus and bulk modulus of composite samples sintered for two hours at various temperatures (1000°C, 1100°C, 1200°C, 1300°C, 1400°C). The elastic properties of materials are generally characterized by Young's modulus, shear modulus, and bulk modulus. In modern materials science, the specific properties of materials have begun to be considered in order to quickly and practically investigate the structure of various materials in order to discover or design new materials with desired properties. In particular, the relationship between the best-known elastic constants Young's modulus, shear modulus and bulk modulus is important, since a sufficient value of modulus of elasticity expressing the ability of a solid to resist external forces will be explanatory in expressing and understanding the internal structure of the material. According to Fig. 6 and TABLE 2, it is seen that ultrasonic modules increase with increasing sintering temperature. At 1400°C, the optimum values of Young's modulus, shear modulus and bulk modulus reached 69.83 GPa, 26.23 GPa and 68.99 GPa, respectively. The density-sintering temperature and microhardness-sintering temperature variation graph was plotted in Fig. 7 using the measured data. Above 1400°C, a significant increase in mechanical performances was observed. This result is also confirmed by SEM micrographs and the known effect of boriding on mechanical strength. It is clearly seen that microhardness and density values are dependent on temperature (Figs. 7a and 7b). Grain growth with increasing sintering temperature increased intergranular porosity and densification, which was eliminated later, increased microhardness and increased durability.

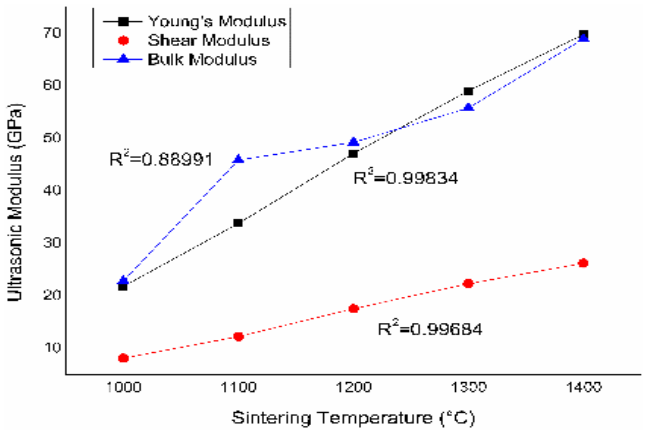

Fig. 6. Relationship between sintering temperature and ultrasonic modulus of ceramic-metal composites

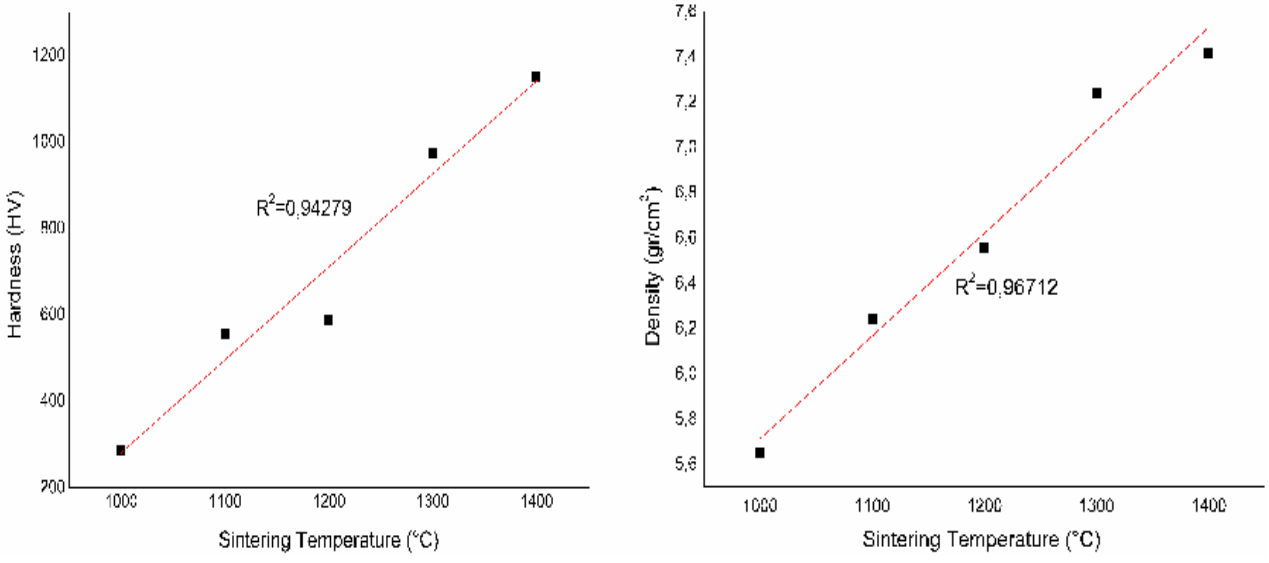

(a) (b)

Fig. 7. Relationship between sintering temperature, microhardness and density of ceramic-metal composites

6. Conclusions

Young's modulus, shear modulus and bulk modulus, (16.59% AlN + 6.63% WC) 76.7Ni composite samples, which were prepared by box boriding after plating with electroless nickel sintered at different temperatures, were evaluated using ultrasonic techniques. The mechanical properties of (16.59% AlN + 6.63% WC) 76.7Ni composites have improved with the increase in sintering temperature and production techniques. Longitudinal and transverse velocities were used to determine the elastic stiffness coefficients of the composites. The calculated values of the mechanical properties prove that (16.59% AlN + 6.63% WC) 76.7Ni composites improve the mechanical properties. At 1400°C, the optimum values of shear modulus, bulk modulus and Young's modulus of (16.59% AlN + 6.63% WC) 76.7Ni composites with different percentages reached 26.23 GPa, 68.99 GPa and 69.83 GPa, respectively. The microhardness value increased and reached 1150.8 HV at the latest. The obtained results showed that the mechanical properties and ultrasonic modulus values of the produced composites were directly related to the sintering temperature. According to the results above 1400°C, it is clearly seen that the microstructure is improved and the effect of boronization.

REFERENCES

[1] A. Yönetken, Fabrication of Electroless Ni Plated Fe–Al_2O_3 Ceramic–Metal Matrix Composites. Trans. Indian Inst. Met. **68** (5), 675-681 (2015).
DOI: https://doi.org/10.1007/s12666-014-0497-1

[2] B. Oraon, G. Majumdar, B. Ghosh, Application of Response Surface Method for Predicting Electroless Nickel Plating. Mater. Des. **27** (10), 1035-1045 (2006).
DOI: https://doi.org/10.1016/j.matdes.2005.01.025

[3] R.C. Agarwala, V. Agarwala, Electroless Alloy/Composite Coatings: A review. Sadhana **28** (3-4), 475-493 (2003).
DOI: https://doi.org/10.1007/BF02706445

[4] Y. Chen, M. Cao, Q. Xu, J. Zhu, Electroless Nickel Platting on Silicon Carbide Nanoparticles. Surf. Coat. Technol. **172** (1), 90-94 (2003). DOI: https://doi.org/10.1016/S0257-8972(03)00320-7

[5] L. Cong, Y. Yanguo, L. Congmin, X. Ming, L. Rongrong, C. Qi, Preparation and Properties of Lead-Free Copper Matrix Composites by Electroless Plating and Mechanical Alloying. Wear **488-489**, 204164 (2022).
DOI: https://doi.org/10.1016/j.wear.2021.204164

[6] R. Ünal, I.H. Sarpün, H.A. Yalım, A. Erol, T. Özdemir, S. Tuncel, The Mean Grain Size Determination of Boron Carbide (B_4C) –Aluminium (Al) and Boron Carbide (B_4C) –Nickel (Ni) Composites by Ultrasonic Velocity Technique. Mater. Charact. **56** (3), 241-244 (2006). DOI: https://doi.org/10.1016/j.matchar.2005.11.006

[7] A. Yönetken, V.Ö. Bilici, Ultrasonic and Mechanical Characterization of Borided Ceramic-Metal Composite. Russ. J. Nondestruct. Test. **58** (9), 779-789 (2022).
DOI: https://doi.org/10. 1134/S1061830922090091

[8] L. Bonin, V. Vitry, F. Delaunois, Inorganic Salts Stabilizers Effect in Electroless Nickel-Boron Plating: Stabilization Mechanism and Microstructure Modification. Surf. Coat. Technol. **401**, 126276 (2020). DOI: https://doi.org/10.1016/j.surfcoat.2020.126276

[9] K. Krishnaveni, N. Sankara, S.K. Seshadri, Electrodeposited Ni–B Coatings: Formation and Evaluation of Microhardness and Wear Resistance. Mater. Chem. Phys. **99** (2-3), 300-308 (2006). DOI: https://doi.org/10.1016/j.matchemphys.2005.10.028

[10] B. Oraon, G. Majumdar, B. Ghosh, Parametric Optimization and Prediction of Electroless Ni–B Deposition, Mater. Des. **28** (7), 2138-2147 (2007).
DOI: https://doi.org/10.1016/j.matdes.2006.05.017

[11] W.P. Ye, Z.L. Huang, Q.X. Zhang, Q.Y. Zhang, Microstructure and of Mechanics Microwave Boriding. J. Wuhan Univ. Technol. Mater. Sci. Ed. **23** (4), 528-531 (2008).
DOI: https://doi.org/10.1007/s11595-006-4528-6

[12] V. Vitry, L. Bonin, Effect of Temperature on Ultrasound-Assisted Electroless Nickel-Boron Plating. Ultrason. Sonochem. **56**, 327-336 (2019).
DOI: https://doi.org/10.1016/j.ultsonch.2019.04.027

[13] J. Krautkrämer, H. Krautkrämer, Ultrasonic Testing of Materials. Springer-Verlag, New York (1990).

[14] G.Y. Li, Z.Y. Zhang, J. Qian, Y. Zheng, W. Liu, H. Wu, Y. Cao, Mechanical Characterization of Functionally Graded Soft Materials with Ultrasound Elastography. Phil. Trans. Roy. Soc. A **377**, 20180075 (2019).
DOI: https://doi.org/10.1098/rsta.2018.0075

[15] Y. Zhao, L. Lin, X.M. Li, M.K. Lei, Simultaneous Determination of The Coating Thickness and Its Longitudinal Velocity by Ultrasonic Nondestructive Method. NDT & E. Int. **43**, 579-585 (2010). DOI: https://doi.org/10.1016/j.ndteint.2010.06.001

[16] A. Kravcov, O.L. Dudchenko, P. Svoboda, P.N. Ivanov, M.V. Sizikov, O.D. Belov, A.A. Gapeev, Broadband Ultrasonic Pulse-Echo Method for Estimation of Local Density of Tungsten Samples. Journal of Physics: Conference Series, V (1172), International Conference on Applied Physics, Power and Material Science 5-6 December 2018, Secunderabad, Telangana, India Citation, J. Phys.: Conf. Ser. 1172, 012064 (2019).
DOI: https://doi.org/10.1088/1742-6596/1172/1/012064

[17] A. Erol, V. Özkan Bilici, A. Yönetken, Characterization of The Elastic Modulus of Ceramic–Metal Composites with Physical and Mechanical Properties by Ultrasonic Technique. Open Chem. **20**, 593-601 (2022).
DOI: https://doi.org/10.1515/chem-2022-0180

[18] N. Bouslama, Y. Chevalier, J. Bouaziz, F.B. Ayed, Influence of The Sintering Temperature on Young's Modulus and The Shear Modulus of Tricalcium Phosphate – Fluorapatite Composites Evaluated by Ultrasound Techniques. Mater. Chem. Phys. **141** (1), 289-297 (2013).
DOI: https://doi.org/10.1016/j.matchemphys.2013.05.013

[19] M. Nazeer, P. Jana, M. Oza Jaydeeokumar, K. Günter Schell, E. C. Bucharsky, T. Laha, S. Roy, Ultrasonic Study of The Elastic Properties of Functionally Graded and Equivalent Monolithic Composites. Mater. Lett. **323**, 132594 (2022).
DOI: https://doi.org/10.1016/j.matlet.2022.132594

[20] Z. Li, Z. Han, X. Jian, W. Shao, Y. Jiao, Y. Cui, Pulse-Echo Acoustic Properties Evaluation Method Using High-Frequency Transducer. Meas. Sci. Technol. **31** (12), 125011 (2020).
DOI: https://doi:10.1088/1361-6501/aba0d8

[21] V.L.A. Freitas, H.C. Albuquerque, E.M. Silva, A.A. Silva, J.M.R.S. Tavares, Nondestructive Characterization of Microstructures and Determination of Elastic Properties in Plain Carbon Steel Using Ultrasonic Measurements. Mater. Sci. Eng. A **527** (16-17), 4431-4437 (2010).
DOI: https://doi.org/10.1016/j.msea.2010.03.090

[22] A.M. El-Taher, S.E. Abd El Azeem, A.A. Ibrahiem, Influence of Permanent Magnet Stirring on Dendrite Morphological and Elastic Properties of a Novel Sn–Ag–Cu–Sb–Al Solder Alloy by Ultrasonic Pulse Echo Method. J. Mater. Sci: Mater. Electron. **31**, 9630-9640 (2020).
DOI: https://doi.org/10.1007/s10854-020-03506-4

[23] X. Wang, C. He, H. He, W. Xie, Simulation and Experimental Research on Nonlinear Ultrasonic Testing of Composite Material Porosity. Appl. Acoust. **188**, 108528 (2022).
DOI: https://doi.org/10.1016/j.apacoust.2021.108528

[24] Q. Li, X. Yang, F. Peng, G. Yang, T. Han, L. Fang, Q. Hu, L. Xie, X. Chen, Y. Zou, Elasticity, Mechanical and Thermal Properties of Submicron h-AlN: in-situ High Pressure Ultrasonic Study. J. Eur. Ceram. Soc. **41** (9), 4788-4793 (2021).
DOI: https:// doi.org/10.1016/j.jeurceramsoc.2021.03.056

[25] R.D. Schmidt, J.E. Ni, E.D. Case, J.S. Sakamoto, D.C. Kleinow, B.L. Wing, R.C. Stewart, E.J. Timm, Room Temperature Young's Modulus, Shear Modulus, and Poisson's Ratio of $Ce_{0.9}Fe_{3.5}Co_{0.5}Sb_{12}$ and $Co_{0.95}Pd_{0.05}Te_{0.05}Sb_3$ Skutterudite Materials. J. Alloys Compd. **504** (2), 303-309 (2010).
DOI: https://doi.org/10.1016/j.jallcom.2010.06.003

[26] K. K. Phani, D. Sanyal, The Relations Between the Shear Modulus, The Bulk Modulus and Young's Modulus for Porous Isotropic Ceramic Materials. Mater. Sci. Eng. **490** (1-2), 305-312 (2008).
DOI: https://doi.org/10.1016/j.msea.2008.01.030

[27] E. Gregorová, V. Nečina, S. Hříbalová, W. Pabst, Temperature Dependence of Young's Modulus and Damping of Partially Sintered and Dense Zirconia Ceramics. J. Eur. Ceram. Soc. **40** (5), 2063-2071 (2020).
DOI: https://doi.org/10.1016/j.jeurceramsoc.2019.12.064

[28] P. Rogl, Phase Diagrams of Ternary Metal–Boron–Carbon Systems. ASM International; MSI, Materials Park, OH; Stuttgart, Germany, (1998), pp. 392.

[29] M. Greenfield, G. Wolfe, Powder Metal Technologies and Applications of ASM Handbook. ASM International **7**, 492-496 (1998).

[30] H.Y. Mehrabani, A. Babakhani, J. Vahdati-khaki, A Discussion on The Formation Mechanism of Tungsten Carbides During Mechanical Milling of $CaWO_4$-Mg-C Mixtures. J. Alloys Compd. **781**, 397-406 (2019).
DOI: https://doi.org/10.1016/j.jallcom.2018.12.066